Adherent and Slippery Walls for Extrusion of Entangled Polymer Melts and Compounds

Jean-Michel Piau

Laboratoire de Rhéologie, Université de Grenoble (UMR 5520-UJF-INPG-CNRS), BP 53, 38041 Grenoble, France

SUMMARY: A brief overview is given of the distortions observed when polymer melts or compounds are extruded. It appears that extrusion through steel dies can be done either with macroscopic slip or with no-slip wall conditions.
Recent experimental and theoretical progress made in understanding the various aspects of slip at the wall, and its measurement techniques, are presented. Boundary conditions for rubber compounds flowing through steel-walled dies could be seen to be much more complex than those for melts. However many aspects of the methodologies developed are of common interest both for melts and rubber.
It has already been suggested that advantages can be obtained from the use of slippery walls in extrusion. Such wall properties have already been used indeed for a long time with compounds, where processing additives are introduced.
New experimental data are presented concerning two typical EPDM compounds series, obtained using several laboratory techniques at the same time. Constitutive equations for the bulk and for friction at the wall can be introduced at present and adjusted to experimental data. Die extrusion can be simulated numerically, and significant improvements can be expected in quality and productivity.

1. Introduction

The processing of polymeric materials involves changes in shape and flow induced by the stresses applied. Hence the products obtained may depend on both the bulk rheometric properties and on the tribometric properties at the wall-fluid interfaces.
Although the possibility of a slip hydrodynamic boundary condition has been considered since the time of Stokes[1)] and Couette[2)], no-slip boundary conditions are currently considered as being relevant for any low molecular mass liquid. In contrast, a slip condition has long been known to apply to gases at low pressures and suspensions as well as to polymer solutions[3-4)], particularly because of the necessary depletion layer at the wall. In some

 CCC 1022-1360/99/$ 17.50+.50/0

problems, advantage is taken of a slip condition to fit a continuum model, although the length scale of the material is not small enough (i.e. less than 1/50) compared to the dimensions of the flow field. Slip is also introduced in metal shaping, because easy-to-shear third bodies appear at interfaces with shaping tools[5-6].

A great variety of situations have been observed for entangled thermoplastics and elastomers[7-10]. Grafted or coated, very smooth or rough surfaces have already been studied in combination with different species of polymers or compounds and different ranges of stress level in simple as well as in complex fields. But the developments to follow will focus on extrusion or capillary flows, and macroscopic slip will be the main point of interest[7-10].

Reviews have been published[11-14] concerning the case of raw elastomer compounds. It is considered that "there must be some slippage of the raw elastomers in an extruder" as, "if this were not the case, the nonmoving stock in contact with the metal would, at the existing temperatures, sooner or later cure"[11]. Compounds retain some of the polymeric component viscoelasticity, but because of active fillers such as carbon black or silica they also show thixotropy and a yield stress. Elastomer slippage, while interesting and proven by visualizations, is normally considered quite slow, so slow that it has apparently proved difficult to obtain direct evidence of slippage or any measurement of it[11]. Two main experimental approaches have been used to calculate slippage: measurements with dies of different lengths and diameters (known as Mooney's method), or measurements from serrated and smooth tools. Power law wall friction formulae have been introduced, with the applied surface shearing stresses increasing typically as the power 1/7 to 1/4 of slip velocity within the data ranges considered. Adding soap to rubber has been found to promote slip, and there is some indication of zinc stearate possibly migrating towards the wall during flow conditions[15].

However, difficulties have appeared with the use of Mooney's method in several studies on ethylene-propylene-diene terpolymer (EPDM) or on styrene butadiene rubber compounds[15-18]. Calculated slip velocity was reported to be higher than the mean flow velocity of the fluid, which is physically impossible. In order to define a correct slip velocity it was suggested that its possible dependence on the die diameter or gap should be considered in addition to the wall shear stress, and "curved" Mooney plots used. This suggestion did not meet with complete success when several die dimensions were used[17].

A possible dependence of the wall friction law on local pressure would generate a non-linear variation in pressure with the abscissa along the die. However, except for pressure and temperature effects on bulk properties, pressure measurements performed along flat dies are reported to be linear with the abscissa [15-17]. It may be noted that a possible influence of pressure on slip data has been reported in rotational rheometers but this may also be related to the influence of ambient pressure on sample shape and fracture inside the rheometer.

It came as a complete surprise when wall slip below a critical shear stress of 1.7×10^5 Pa was reported for two EPDM compounds, and no slip above the critical wall shear stress[16]. No-slip was explained using a microstructural model where wall roughness asperities penetrate the compound at high stress levels only, and this was associated with an apparent independence of the flow curves with respect to the gap inside the extrusion die. A closer look at the difficulty of the experiments and the precision of the data obtained, and at the limited range of dies used suggests that this point needs further consideration.

The purpose of the present work is to review and amplify current understanding of macroscopic slip at the wall, as it is most useful for polymer and rubber compound extrusion.
Guidelines are necessary before studying any new extrusion process and it is quite difficult to avoid all the traps[19]. Observation of extrudate distortions offers useful indications and this will be examined together with slip measurement techniques in section 2. In section 3, it will be shown how the situation at hand for compounds can be modelled in simple terms from available friction formulae and the constitutive equations for yield stress fluids. Finally, recently obtained experimental data are given in section 4 and compared with the theoretical model. The main conclusions will be drawn in section 5.

2. Extrudate distortions and slip velocity measurements.

Complex distortions may appear in all stressed material samples, whatever the experimental system used. This is particularly the case for extrusion, where some of the possible distortions are controlled by slip phenomena or are superimposed on slip.

2.1. Key phenomena in instabilities and extrudate distortions

Instabilities and extrudate distortions offer many facets, as can be seen at once from the great number of possible situations which have been identified in Tab.1. Though each particular situation may show minor differences, all are due to combinations of a series of physical properties common to all the polymeric materials and die walls considered: viscosity, plasticity, viscoelasticity, slip, adhesion, compressibility, fracture and localization, migration and phase changes.

Tab.1. Extrusion flow instabilities

Upstream zone instability (generates extrudate heterogeneity and buckling)
- corner and lip vortex discharge
- upstream viscoelastic instability (i.e. melt fracture initiation)
- upstream deformation localizations
Fluid-die land wall interactions
- slip on slippery walls (smooth, low-energy, grafted, coated, coextruded, immiscible)
- slip on a thin coextruded layer
- slip on high-energy and on rough surfaces
- 1st and 2nd oscillating flows
- flow rate jumps
- material fracture along the die land (i.e. peeling)
Exit zone
- detachment point instability
- extrudate surface cracking (i.e. sharkskin)
- die drool
- extrudate mechanical heterogeneity
- extrudate buckling (i.e. extrudate melt fracture)
- die swell
- unbalanced die extrudate distortions
Downstream
- extrudate relaxation
- draw resonance
Thermodynamics
- flow crystallisation
- migration of the components in flow conditions
- fluid compressibility
- internal stresses and slip friction power dissipation
- influence of state parameters on material functions

2.2 Slip velocity measurement techniques

Let us consider the particular case of the fully developed Poiseuille flow in a tube of diameter D. Given the apparent viscosity function of the material, wall slip velocity U_S as well as non-slip boundary conditions can be used to integrate the shear rate shear stress law $\gamma(\tau)$ and find the mean flow velocity U dependence in the wall shear stress τ_w:

$$8\,\frac{u - U_S}{D} = \frac{4}{\tau_w^3}\int_0^{\tau_w} \tau^2\gamma(\tau)d\tau \qquad (1)$$

Usually the apparent wall shear rate is introduced by extending Newtonian relationships with adhesion, and it is defined as:

$$\gamma_{app} = 8\,\frac{u}{D} = 32\,\frac{Q_v}{\pi\ D^3} \qquad (2)$$

Similar formulae can be written for cylindrical tube section shapes that are not circular.

These are the basic equations used for rheometric measurements and for flow calculations. Several important simplifying hypotheses are used, and these must be clearly indicated, though they may prove to be difficult to fulfil simultaneously and inconsistencies may result:

- the flowing material can be modelled as a single monophase continuum, whatever the flow intensity,
- temperature and pressure have negligible influences on material functions, and dissipation is neglected
- the flow field is steady, laminar, and isochoric,
- only wall shear stress values are considered for long dies; these must be calculated far enough from the entrance and the exit zone. In particular, Couette-Bagley correction for the entrance pressure drop enables the correspondence between measured linear pressure drop and τ_w to be established.

Equation (1) can be used to discover several methods for measuring slip velocity and deducing friction curves. It is important to recall that it is not always easy to produce conditions where it is valid, and this must be checked.

The first method is derived from the assumption made by Mooney that the slip velocity depends only on the local wall shear stress: $U_S = U_S(\tau_w)$. Thus for a given value of the wall shear stress, a plot of the apparent shear rate against the reciprocal diameter D^{-1} yields a straight line with a slope equal to eight times the value of the slip velocity (the most commonly used coefficient is 4 for the reciprocal die radius). By repeating this procedure for successive values of τ_w it is possible to draw the wall friction law $\tau_w(U_S)$.
This method has been tentatively extended recently using the assumption that the slip velocity depends on the die diameter as well as on the local wall shear stress[15-16]: $U_S = U_S(D, \tau_w)$.

A second method can be introduced when the apparent viscosity function is available from independent rheometric measurements, obtained for instance using a rotational rheometer. The integral in equation (1)'s right term can then be calculated for any particular value of the shear stress. If the extrusion data give the mean flow velocity for this same shear stress value, the associated slip velocity and the wall friction law can be deduced again from equation (1). Difficulties may arise from obtaining correct values of the apparent viscosity, without undue extrapolations, and without slip or fluid fracture errors in the devices used.

A third method results from situations where slip or no-slip conditions at the tube wall can be controlled by specific chemical preparation of the surface or by using serrated surfaces. A given flowing material submitted in a given tube geometry to a given applied wall stress corresponds to a constant value of the right term in equation 1). If the experiment is performed successively with slip and with no-slip boundary conditions, the difference in the measured flow rate enables the slip velocity U_S to be deduced for the given shear stress value τ_w. This will be the difference between the mean velocities calculated with slip U_S and with no-slip U_{ns}: $U_S = U_S - U_{ns}$.

The last two methods to follow consist of direct velocity measurements. It is interesting to note that they have no connection with equation (1). Nevertheless one may wish to introduce velocity data in (1).
The fourth method is the direct measurement of local slip velocity from the displacement of particles added to the fluid or already present (and possibly of the stress value at the wall using birefringence of transparent fluids).

Advantage can be taken of available video, chronophotography, laser Doppler velocimetry, or particle image velocimetry techniques. The main difficulties arising from the need for a very local velocity probe in the wall region, where high shear gradients prevail.

The fifth method consists in marking the material without adding visible particles. Molecular probes or physico-chemical treatments of the components may allow velocity to be deduced within submicronic distances from the wall. Fluorescence bleaching[20] of a melt has already been triggered very locally over a short distance from the wall and slip velocity has been deduced by following the displacement of the bleached zone in time. Alternatively, the local decay of fluorescence[21] when a fluorescent material layer initially coating the wall is displaced by the same non-fluorescent material, provides useful information about the velocity field near the wall. The main difficulties may arise from flow field control and drift in the mechanical properties of the fluid in apparatuses and fluids that must fit the marking technique.

3. Flow modelling with macroscopic slip friction and plasticity.

It is possible to take advantage of equations that are already available for the bulk and wall behaviour of polymer melts, and of equations for the bulk properties of viscoplastic materials. On this basis, it is possible to suggest a simple overall theory that may be very useful before proceeding to very difficult experimental measurements and data interpretations concerning compounds. In addition, this same theory can also be worked into a numerical code to obtain a more detailed flow description, as will be shown in this section.

Extrusion of compounds is governed by their viscoplasticity and their ability to slip at the walls of dies. The behaviour of metals and ceramics is similar.

Hence a Herschel-Bulkley model can represent bulk rheometric properties at the die entrance, and within the flowing media sheared inside. Friction laws already used in the field of polymer melts and cured rubber can represent boundary properties. At wall shear stress levels smaller than the yield value there is no flow at all for no-slip conditions, and flow is possible only if it is permitted by the friction laws and entrance bulk stresses. At high wall shear stress levels, flow results from a combination of slip at the wall and shearing in the bulk. Hence there is a big difference in comparison with the case of viscous or viscoelastic polymer melts, where flow and shearing in the bulk exist whatever the wall shear stress level, and friction laws allow slip to occur only

when a critical shear stress is overcome in usual extrusion conditions without additives.
The pressure head applied upstream is used in part to generate tube entrance flow, bulk dissipation inside the tube, if any, and for the wall friction term[10].
As in equation (1) the mean flow velocity inside the tube U is a combination of two contributions: one from the sheared material U_{vp} if any, and one from the slip velocity Us.

The Hercshel-Bulkley model can be written in its scalar form for a shear flow, giving the shear stress value τ versus shear rate value γ and two parameters n and k: $\tau = s + k\gamma^n$.
The mean flow velocity U_{vp} inside a tube of diameter D can be calculated exactly according to the value of the shear stress τ_w at the wall:

- if $\tau_w = s$ then $U_{vp} = 0$ (3)

- if $\tau_w > s$ then $u_{vp} = \frac{(1-a)^{m+1}}{2(m+3)} \left(\frac{s}{a\,k}\right)^m wD$ (4)

$$\text{where } a = \frac{s}{\tau_w} \qquad \text{and } w = 1 + \frac{2\,a}{m+2} + \frac{2\,a^2}{(m+1)(m+2)}$$

Inertialess tube entrance flow for a Herschel-Bulkley model is not completely understood at the present time. However, certain indications for power law viscous models[22] and from ceramics and the field of metals where extrusion is done from an upstream reservoir[23] of diameter D_u can be used to suggest the following approximation for the entrance zone pressure head loss ΔPe:

$$\Delta Pe = 2\ \log\frac{D_u}{D}\left(s\sqrt{3} + \ 4\ \ k\left(6 + \frac{2}{n}\right)^n (0.58 - 1.44\log n)\left(\frac{u}{D}\right)^n \right) \quad (5)$$

In the following discussion, this will be applied to a long enough die. The first term, proportional to the yield stress, helps in solving the low flow rate. The viscous term will be ignored temporarily.

Two models[24-26] have already been used successfully to model the friction stress τ_w versus slip velocity Us of polymer melts and rubber, depending on whether it was necessary to model high velocity instabilities (6) or not (7):

$$\tau_w = \tau_s + Ae^{-\lambda U_s} + B\frac{1-(1+\alpha+x)e^{-\alpha-x}}{x(1+\alpha\beta-e^{-\alpha-x})} \quad (6)$$

$$\tau_w = \tau_s + Ae^{-\lambda U_s} + B\frac{1-e^{-x}-xe^{-x}}{x(1+\alpha-e^{-x})} \quad (7)$$

where $x = \frac{U_a}{U_s}$, U_a being a reference velocity used to adjust the value of the slip velocity corresponding to the maximum of the friction curve, α is used to adjust the curvature of the bell-shaped part of the friction curve and β its second minimum, A, λ, and τ_s adjust the lower velocity part of the friction curve.

For every given value of Us, it is possible to deduce the wall shear stress τ_w and U_{vp} from the equations above, as suggested in Tab. 2. The mean velocity U is then calculated by adding the previous two velocities.
The given shear stress τ_w corresponds to a pressure head loss within the capillary of $\Delta Pc = \frac{4L}{D}\tau_w$. Since equation (5) gives the entrance pressure head loss, the total pressure head is found to be $\Delta P = \Delta Pc + \Delta Pe$.

Tab. 2. Calculation procedure.

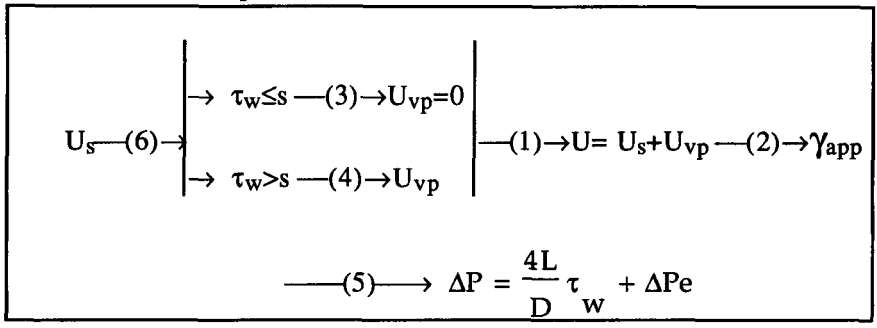

Flow curves can be constructed. It may be noticed that some very interesting stability and unicity questions may appear depending on the values given to the parameters (two oscillating regions have already been reported, and photographs have been published for a polyethylene[10]).

A set of parameters was chosen to draw curves describing the flow properties. The following set will be shown to be relevant in section 4 of this paper: $s=2x10^5$ Pa, Du/D=10, L/D=20/2 (mm) for all applications except the last one where L/D=10/1 will also be considered, m=3, k= 10^4 Pa.$s^{1/3}$, B= $8x10^5$ Pa, $a=5x10^{-4}$, U_a=0.01 or 0.1 m/s, $\tau_s=2x10^4$ Pa, A=0.

Fig. 1 gives the useful part of the two bell-shaped friction curves obtained. They are translated into a log scale along the abscissa when Ua is changed. For zero Us, τ_w tends towards τ_s. The critical value Usc of slip velocity Us is obtained when τ_w is exactly equal to the yield value s. For all values of slip velocity less than or equal to Usc there is no shearing contribution to the rate of flow, and the mean flow velocity is equal to the slip velocity. When such conditions are known to occur, slip velocity is easy to obtain.

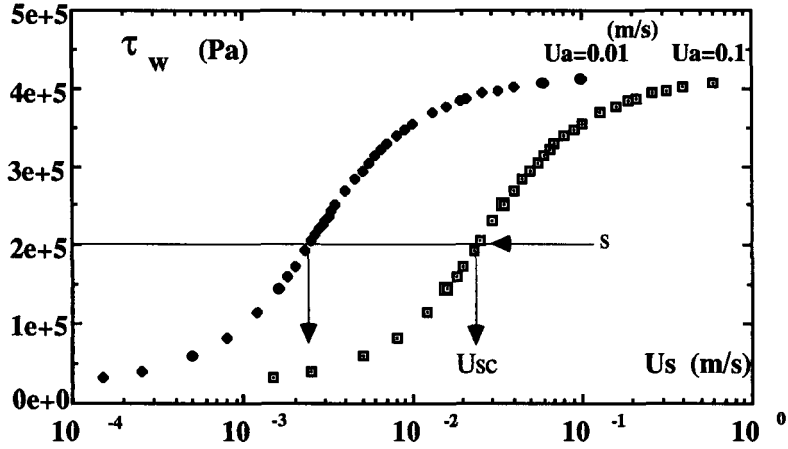

Fig. 1. Friction curves: variations in shear stress τ_w versus slip velocity Us.

The total pressure drop ΔP is one of the most accessible experimental properties. Its variations with the rate of flow or equivalently the apparent shear rate γ_{app} are given in Fig. 2 . For very small values of the rate of flow ΔP tends towards a limit fixed by the yield stress value s and non-zero τ_s:

$$\Delta P_0 = \frac{4L}{D}\tau_s + 2\sqrt{3}\ s\ \log\frac{D_u}{D} \qquad (8)$$

i.e. 1.5 x 10^6 Pa in the present application.

Two different flow regions seem to be distinguished since some change in slope occurs on the graph. It also appears that the upper parts of the curves have a slight slope and then bend, as seen from some data with a thermal effect, though there is none in our isothermal model.

The boundary between the two flow regimes is exactly determined by the value Usc of the critical slip velocity, which has been defined on Fig. 1.

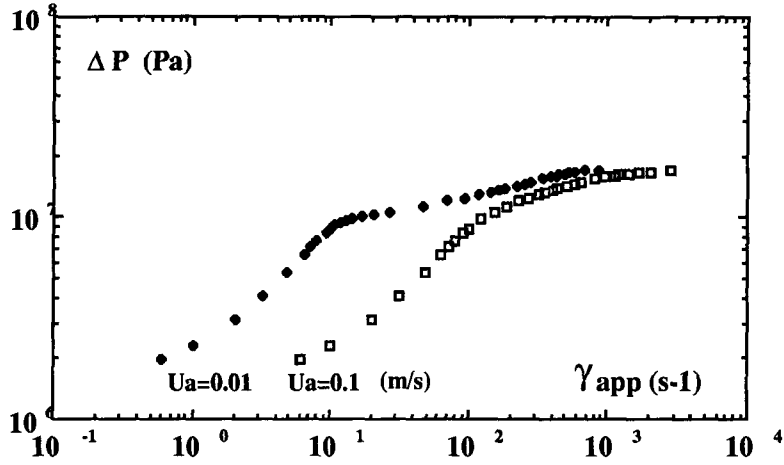

Fig. 2. Total head pressure drop ΔP versus apparent shear rate γ_{app}.

After the Couette-Bagley correction has been made, it is quite common to draw the graph of shear stress variations at the wall of the tube versus apparent shear rate. Fig. 3 gives the results obtained from the present model. Two different flow regimes may again appear (slip without shear and slip with shear) depending on slip velocity and shear stress conditions, as compared to the values of velocity Usc and yield stress s. There is clear evidence that slip dominates the model curves at low shear rates.

A rheogram, i.e. a curve typical of the bulk properties for a yield stress fluid, obtained for no-slip conditions, is also plotted on the same graph. This rheogram can be closely superimposed at high shear rate upon the curve with reference slip velocity Ua=0.01 m/s. This means that slip is dominated by shear in this regime. However it is clear that the merging of the two curves does not mean we have no-slip conditions. This merging would also appear for other values of the die diameter, and it should be noticed that there is little apparent influence of the die diameter at high rate of flow, though slip boundary conditions apply.

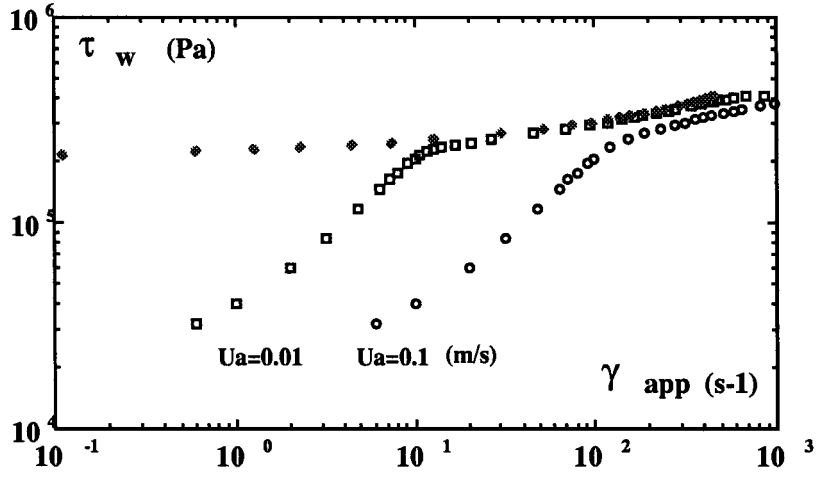

Fig. 3. Rheogram and curves with slip for shear stress versus apparent shear rate

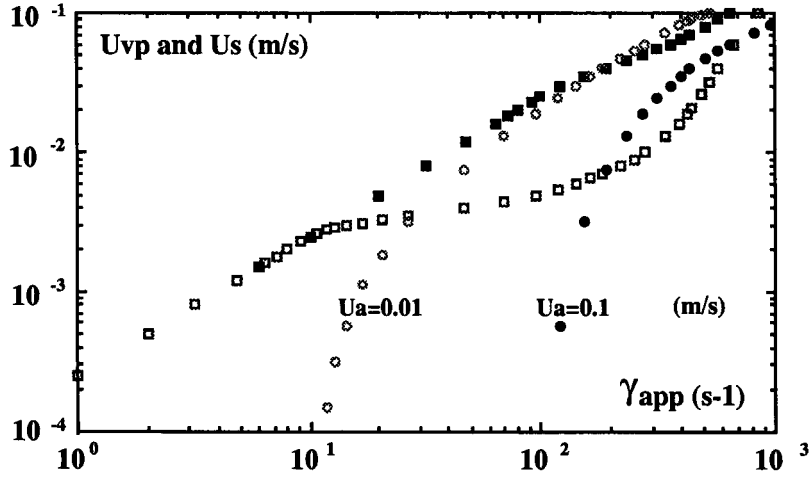

Fig. 4. Mean shear velocity U_{vp} and slip velocity Us versus apparent shear rate γ_{app} for two values of Ua. Open symbols are used for Ua= 0.01 m/s and black symbols for Ua= 0.1 m/s.

The rate of flow through a capillary is a combination of two contributions. One is due to slip, while the second is related to the shearing of the yield stress fluid at the wall. Fig. 4 displays each of the two contributions using mean velocities through the capillary. When Ua=0.1 m/s, the two curves with the

black dots do not overlap, and though the shearing term U_{vp} increases rapidly, slip velocity Us remains greater. The other case for Ua=0.01 m/s shows that the shearing term is indeed the greater at a high rates of flow, as expected from Fig. 3.

It is common to consider that the weak influence of the die diameter is the crucial point for deciding that no-slip prevails when using a shear stress-shear rate graph such as Fig. 5. The chosen conditions are favourable for finding a diameter effect on the graph, since Ua=0.1 m/s and the shear term is dominant at high rate of flow, and since the die diameters used are in a ratio of one to two (something which has not always been possible in experiments where the dies used may differ only by a few tenths). Nevertheless the model shows how it may be tempting to decide that there is no slip in an experiment at high rate of flow, despite the fact that it is the dominant phenomenon. The difficulty is enhanced by the slight slope of the curves in the region considered.

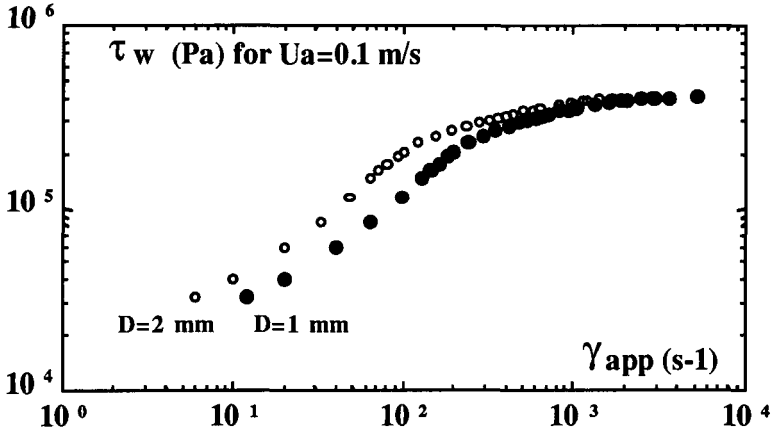

Figure 5. Influence of die diameter on a shear stress-shear rate plot.

By introducing the theoretical formulae of section 3 into an appropriate software, together with parameters adjusted to fit the experimental data from section 4 below, it is possible to predict many different flow situations. As a simple example[27] the two principal stress difference charts reproduced in Fig. 6 show how much the plots can differ for the same apparent shear rates (i.e. the same mean rate of flow) with and without slip boundary conditions.

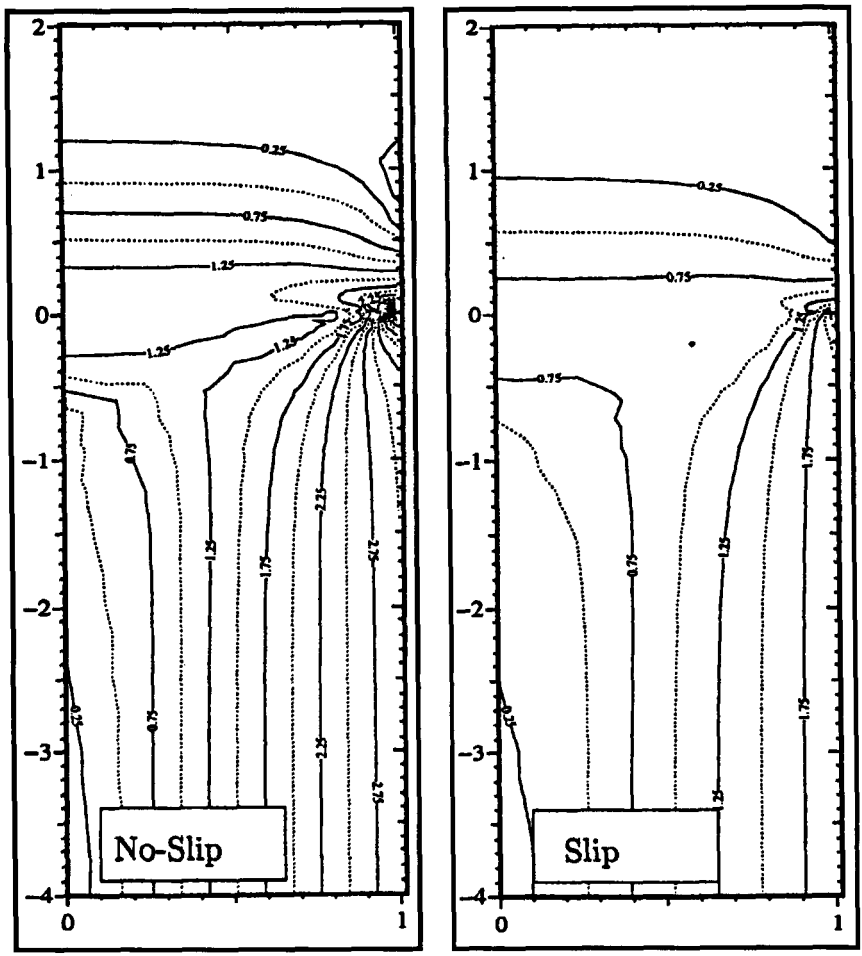

Figure 6. The flow of a polydimethylsiloxane melt is modelled using a Bird-Carreau model and a friction law similar to equation (7). First principal stress difference charts correspond to γ_{app}= 16 s^{-1} in an axisymmetric die.

4. Combined slip measurements and mechanisms for compounds

4.1. Elastomers and compounds studied

Two typical EPDMs were chosen, with significantly different slip behaviours, due to different molecular weight distributions. EPDM A does not slip in steel dies. It is moderately entangled. EPDM B slips at wall stress levels greater than 0.3 MPa in steel dies.

Two compound formulae studied[28] are given in Tab. 3. Compound A83 is typical of compounds prepared for injection moulding, and compound B158 is typical of extrusion processes.
When the amount of carbon black in compound A83 formula is changed to 60, 40, 20, 10 g, the corresponding samples are designated by A60, A40, A20, A10.
When the processing agents are eliminated the above formulae become A83S, A60S, A40S.
Following the same designation rules as for compound A, samples of compounds B158 and B100, B158S were also studied.

Tab. 3. Formulation of EPDM compound (in grams, or in parts).

EPDM A and compounds A83	
EPDM Mw=260 000	100 g
N550 carbon black	83 g
Processing agents	4.5 g
Zinc oxide and others	8.5 g
Processing agents include zinc stearate, polyethylene wax, and soap.	
EPDM B and compounds B158	
EPDM (high Mw)	100 g
N550 carbon black	158 g
$CaCO_3$	40 g
Oil	96 g
Processing agent (stearic acid)	1 g
Zinc oxide and others	8.8 g

4.2 Experimental set-ups and characterization techniques

Two Goettfert 2001 and 1500 rheometers with a 12 mm barrel were used. They were equipped either with smooth tungsten carbide, or with steel, or with silica glass dies. Dynisco pressure transducers were used. The temperatures of the metal parts, including that inside a hole drilled in the metal dies, were measured using thermocouples. The temperature of the extrudate surfaces close to the outlet was measured with an infrared sensor, and the temperature inside the extrudates was obtained using a home-made thermocouple.
A series of steel capillary dies were serrated[29] using taps, with final hydraulic diameters equal to 1.02 and 1.86 mm. Most of the metal dies used were

available in L/D=5, 10, 20, 30 length to diameter ratios. Orifice dies were also used. A home-made temperature regulated die, with an electric heating unit and a valve could be bolted on the exit from classical dies to create a variable mean pressure level at will, and to measure the influence of pressure on viscosity.
An L/D= 30/2 (mm) steel die made of two semi-circular bolted parts was used to analyse chemical components at the die wall more easily.

The temperature was regulated by circulating air around the transparent 5/2, 10/2, 20/2, 20/3 silica glass dies, which were enclosed inside a glass tube with the necessary holes. Complete visual observations of the flow from the upstream reservoir to the free surface jet, including the capillary itself were made using a Leitz macroscope, as well as a video system and a zoom. In addition, direct chronophotography and laser Doppler velocity measurements were performed on the opaque compounds moving along the die lands through the transparent die walls, using a Dantec laser Doppler velocimeter. Measured velocities were considered to be equal to slip velocity.

A Haake Rheocord could be equipped with either a 1x10x100 or a 0.5x10x100 (mm) steel slit die and three flush pressure transducers.
A rotational Rheometrics RMS 800 rheometer with home-made serrated tools, a TMS Rheometer, and a modified Mooney rheometer were used.

Extrudate distortions were observed either at the die outlet or on relaxed extrudates, using a macroscope, a video system, or scanning electronic microscopes (SEM). Chemical components on the extrudate surfaces and the surface of the circular die, which can be dismantled, were analysed when possible using infrared spectroscopy (limited to 40 parts carbon black), as well as back-scattered electrons and X-ray detection SEM. Dithizone titration following acetone extraction enabled zinc concentration on the extrudate surfaces to be monitored.

4.3 Experimental results

All the data obtained for EPDM A and B are similar to those already obtained for polymer melts[10]. The flow curves obtained for the compounds are typical of yield stress fluid rheometry and look like curves drawn on Fig. 2. The values of the critical velocity Usc and yield stress s indeed appear on shear stress-shear rate graphs. The values found are (25 mm/s, $7x10^5$ Pa) for

compound A, and (7.5 mm/s, 2x10^5 Pa) for compound B. The influence of die diameter is an evident indication of slip for low stress levels, but this may seem ambiguous indeed to the experimenter at high stress levels, as already visualized on Fig. 3 and 5.
Velocity measurements were performed using all five methods suggested above and friction curves were obtained. In fact methods 2 and 3, 4 and 5 coincide, hence only three curves are displayed on Fig. 7 for the case of compound A83. All the measurements show a good agreement except at high slip velocity values (corresponding to large flow rates) where the general trends of the friction curve are lost when using Mooney's method. Friction in the smooth glass die is very slightly lower than in a steel die for the smallest slip velocities only.

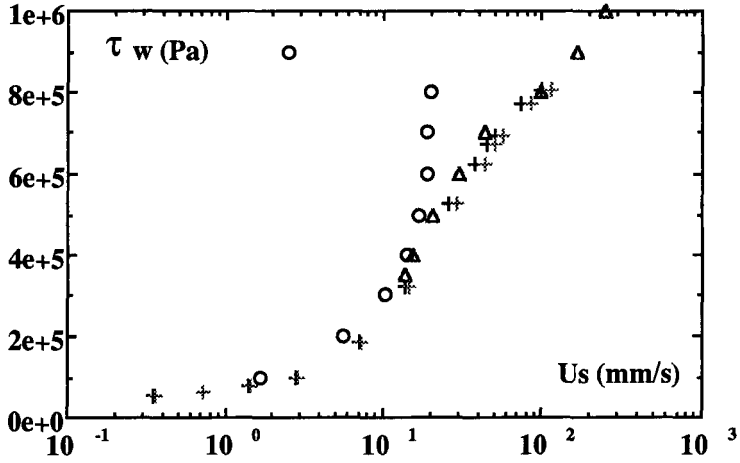

Fig. 7. Friction curves obtained at 100°C for compound A. (+) direct laser Doppler velocimetry inside a 20/2 glass die. (Δ) deduced from rough and smooth 5/1 steel dies measurements. (O) deduced from Mooney's method applied to L/D=5 steel dies data.

The influence of compound formulation and carbon black concentration on friction curves is given in Figs. 8 and 9. Hard and reinforcing carbon black particles increase friction stress for comparable slip velocity values.
In Fig. 9, EPDM B is found to slip at the wall for shear stress levels higher than a critical stress level. A minimum appears in the friction curve ,

generating typical instabilities[10]. Comparison with compound B100 shows the major influence of compound formulation in lowering the slippage critical stress level and friction stress values. In addition the minimum is seen to disappear.

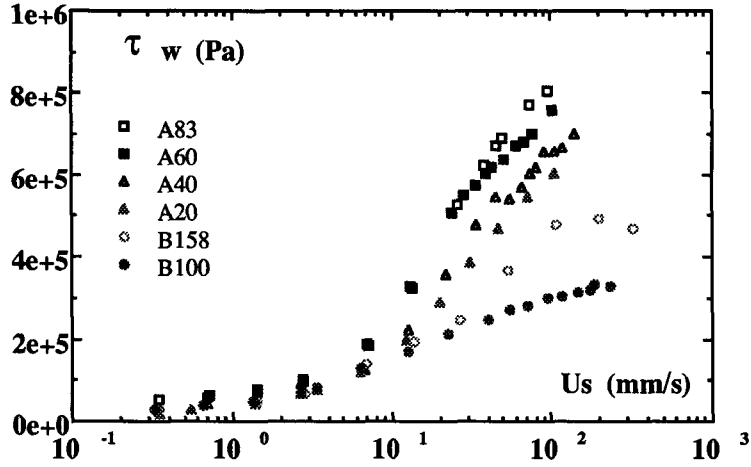

Fig. 8. Friction curves obtained at 100°C in a 20/2 glass die. Influence of compound formulation.

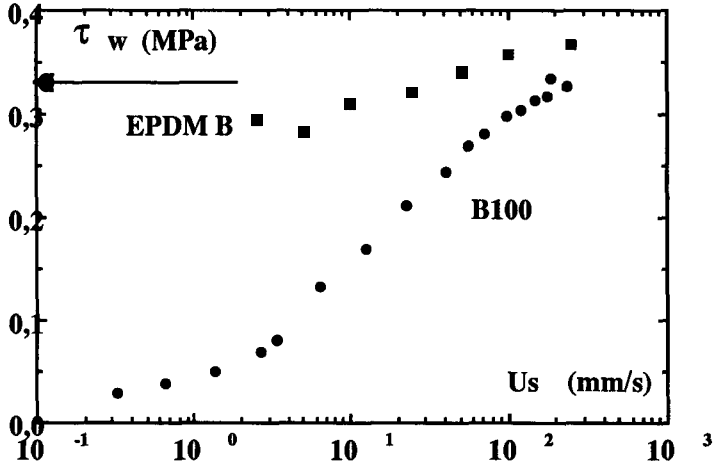

Fig. 9. EPDM B and compound B100 friction curves at T=100°C, measured in a smooth L/D=20/2 glass die. The glass die used for studying EPDM B was clean and free of processing additives.

Chemical analysis proves that processing additives, and particularly soap, migrate towards the die walls under flow conditions. A lubrication regime is created with a lubricating third body between the compound and the wall, and the adhesive component of friction is drastically reduced.
The extrudate distortions observed on EPDM A and EPDM B are exactly the same as expected from polymer melt studies on moderately and on very entangled melts[10]. Reinforced A and B compound series flow with slip at the wall and they mainly show cracks at the die outlet, the dimensions of which depend on the compound formulation and stresses applied. Crack dimensions appear to be reduced by adding processing agents (friction stresses are smaller) and by increasing carbon black content (the compound is stronger).

5. Conclusions

Recent results obtained for polymer melts and for compounds provide a better understanding of extrusion processes, including possibly macroscopic slip at the wall.
Slip velocity and friction curves can indeed be measured or calculated correctly thanks to a series of techniques. The data found can be represented by theoretical formulae. But simple power laws for friction versus slip velocity are not really relevant, while bell-shaped friction laws similar to that used for cured rubber[30-31] are to be preferred for polymer melts as well as for compounds.
Numerical modelling can be performed using a finite-element software and appropriate boundary conditions. It is currently possible to calculate 3D die flows reasonably well, and to take advantage of modelling tools in order to reduce die tuning times significantly.
The results found and the physical phenomena concerned are general enough. They can be extended to other materials and processes.

References

1) G.G. Stokes, *Trans. Cambridge Philos. Soc.* **8**, 287 (1845)
2) J.M. Piau, M. Bremond, J.M. Couette, M. Piau, *Rheol. Acta*, **33**, 357 (1994).
3) J.G. Oldroyd, in F.R. Eirich ed., *Rheology* vol 1, Academic Press, New York, 1956, p 653
4) Y. Cohen, *Encyclopedia of Fluid Mechanics* Vol 7, N. P. Cheremisinoff, ed., Gulf Pub. Co., Houston, 1988, Chap 14

5) D. Dowson, C. Taylor, T. Childs, G. Dalmaz ed., *Lubricants and lubrication,* Tribology Series, 30, Elsevier, Amsterdam, 1995.
6) D. Dowson ed., *Wear a celebration volume*, Elsevier Sequoia S.A., Lausanne, 1985.
7) J-M. Piau and J-F. Agassant ed., *Rheology for Polymer Melt Processing*, Elsevier Science B.V.,1996
8) C. J. S. Petrie and M. M. Denn, *AIChE Journal* , **22**, 209 (1976)
9) E. Boudreaux and J.A. Cuculo, *J. Macromol. Sci.-Rev. Macromol. Chem.* C11(1), 39 (1977).
10) J.M. Piau., N. El Kissi, F. Toussaint and A. Mezghani, Rheologica Acta, 34, 40 (1995)
11) M. Mooney, *"Rheology, theory and applications"*, edited by F.R. Eirich, Acad. Press Inc. Publishers, New York 1958, p. 181
12) J.L. White, *"Science and technology of rubber"*, edited by J.E. Mark, B. Erman, F.R. Eirich, Acad. Press Inc. Publishers, 1994, p.257
13) J. Leblanc, *"Rhéologie des élastomères"*, Artel, Namur, 1996
14) A.D. Roberts, *"Natural rubber science and technology"*, Oxford University Press, 1988
15) S. Wiegreffe, *Kautsch Gummi Kunstst.* **44**, 216 (1992)
16) K. Geiger, *Kautsch Gummi Kunstst.* **42**, 273 (1989)
17) Ph. Mourniac, J-F. Agassant, B. Vergnes, *Rheol. Acta*, **31**, 565, (1992)
18) B. Vergnes, S. d'Halewyn, M-F. Boube, in *Theoretical and Applied Rheology*, P. Moldenaers and R. Keunings ed., Elsevier Science Pub., 1992, p. 399
19) J-M. Piau, N. El Kissi, in *Theoretical and Applied Rheology*, P. Moldenaers and R. Keunings ed., Elsevier Science Pub., 1992, p. 70
20) Migler K. B., Hervet H., Léger L., *Phys. Rev. Lett.* **70**(3), 287 (1993)
21) F. Legrand, J-M. Piau, H. Hervet,*Journal of Rheology*, in press(1998)
22) D.V. Boger, *Advances in Transport Processes*, vol 2, 1982, p. 43
23) J. Zheng, W.B. Carlson, J. Reed, *J. of the Amer. Ceram. Soc.*, **75**, 3011, (1992)
24) J.M. Piau, N. El Kissi, *J. Non-Newtonian Fluid Mech.*, **54**, 121 (1994)
25) Y. B. Chernyak, A.I. Leonov, *Wear*, **108**, 105 (1986)
26) A.I. Leonov, *Wear* **141**, 137 (1990)
27) P. Jay, N. El Kissi, J-M. Piau, J. Cizeron, *J. Non-Newtonian Fluid Mech.*, in press (1998)
28) A. Mezry, PhD Dissertation, INPG Grenoble, 1995.
29) K. Funatsu, T. Kajiwara, *Encyclopedia of Fluid Mechanics* Vol 7, N. P. Cheremisinoff, ed., Gulf Pub. Co., Houston, 1988, Chap 13
30) D. F. Moore, *The friction and lubrication of elastomers* , Pergamon Press, 1972
31) M. Barquins, A.D. Roberts, *J. Phys. D. Appl. Phys.*, **108**, 105 (1986)